Degradation of 'Lumarith' Cellulose Acetate

EXAMINATION AND CHEMICAL ANALYSIS OF A SALESMAN'S SAMPLE KIT

Jia-sun Tsang, Odile Madden, Mary Coughlin, Anthony Maiorana, Judy Watson, Nicole C. Little and Robert J. Speakman

Objects manufactured from cellulose acetate comprise one of the most problematic groups of plastic in the collections of the Smithsonian Institution's National Museum of American History (NMAH). To understand better cellulose acetate degradation, a 'salesman's sample kit' of 'Lumarith' brand, injection-molded, cellulose acetate color samples, manufactured by the Celluloid Company in the early twentieth century and now in the NMAH collection, was studied using minimally invasive analytical techniques at the Smithsonian Institution's Museum Conservation Institute (MCI). The kit includes 49 plastic coupons that vary in color, transparency, chemical composition and current state of degradation. Results of analysis were compared with Celluloid Company records at the NMAH Archives Center and Celanese Corporation in Narrows, Virginia, in order to determine the causes for their current level of preservation or degradation. The possible reasons for the degradation of some coupons are discussed; methods are proposed for identifying cellulose acetate objects that are at risk and for early detection of degradation.

INTRODUCTION

The plastics industry is now in its second century and plastic materials are increasingly common in both museum and fine art collections. As more and more of these objects begin to exhibit signs of degradation, plastics are facing scrutiny about their permanence and the potential of deteriorating objects to contaminate the surrounding collection through the release of degradation products. A year-long survey of plastic objects at the Smithsonian Institution's National Museum of American History (NMAH) [1] determined that the most common plastics in the collections are cellulose nitrate, cellulose acetate (cellulose ethanoate), polyvinyl chloride (polychloroethene), polyurethane, rubber and phenol formaldehyde (phenol methanal). These plastics, with the exception of phenol formaldehyde, are termed 'malignant' [2], because their deterioration products can adversely affect other materials, including paper, metal and other plastics that may be stored in the immediate vicinity. Thus, it has become crucial to identify these malignant plastics and investigate the causes of their deterioration. Many factors may influence the state of preservation of such materials, including their chemical composition, the manufacturing processes by which they were created, as well as their subsequent history of use, collection, conservation treatment, storage and exhibition.

NMAH has in its collection an early salesman's marketing and promotion sample kit of 49 colored, injection-molded 'Lumarith' coupons that are strung together on a beaded metal chain (Figure 1). Lumarith was an injection-moldable cellulose acetate plastic produced by the Celluloid Corporation beginning in the mid-1920s. The Lumarith coupons are identical in shape and size and appear to have been manufactured by the same injection-molding process. It is assumed that the coupons have remained together on the metal chain since their manufacture and, consequently, share a common history. However, the coupons differ in their composition and current state of preservation. As the Lumarith sample kit offers an excellent case study of naturally aged cellulose acetate coupons that were manufactured in the 1920s or 1930s, Museum

Received March 2008

Figure 1 *'Lumarith' (cellulose acetate) color samples kit manufactured in the late 1920s or 1930s. The sample kit consists of 49 coupons, each roughly 3.8 × 6.3 cm, looped on a 35 cm metal chain. Coupons have aged differently through time: some are in good condition, some samples exhibit signs of deterioration and some have undergone advanced deterioration.*

Conservation Institute (MCI) staff were granted a two month loan of the object with permission to conduct a technical study using non-destructive techniques (with one exception, discussed below). This loan provided a rare opportunity to study the effects of chemical composition on the long-term stability of three-dimensional, injection-molded cellulose acetate objects with a limited number of experimental variables.

The coupons and their connecting metal chain were examined visually, using both the unaided eye and magnification to understand the process by which they were manufactured and to assess their current state of preservation. The dimensions and weight of each sample were measured. Information about the molecular structure of the plastic components was obtained by Fourier transform Raman spectroscopy (FT-Raman) and Fourier transform infrared spectroscopy (FTIR). Elemental data were generated using X-ray fluorescence spectroscopy (XRF) and scanning electron microscopy with energy-dispersive spectroscopic (SEM-EDX) mapping. X-ray diffraction (XRD) was performed on a small white crystal from the metal chain.

Of the 49 coupons in the sample kit, 31 did not show any signs of degradation (Figure 2). Some signs of degradation were shown by 18; three of these were severely degraded (Figure 3). The condition of the coupons was found to correlate strongly with the presence of triphenyl phosphate (TPP).

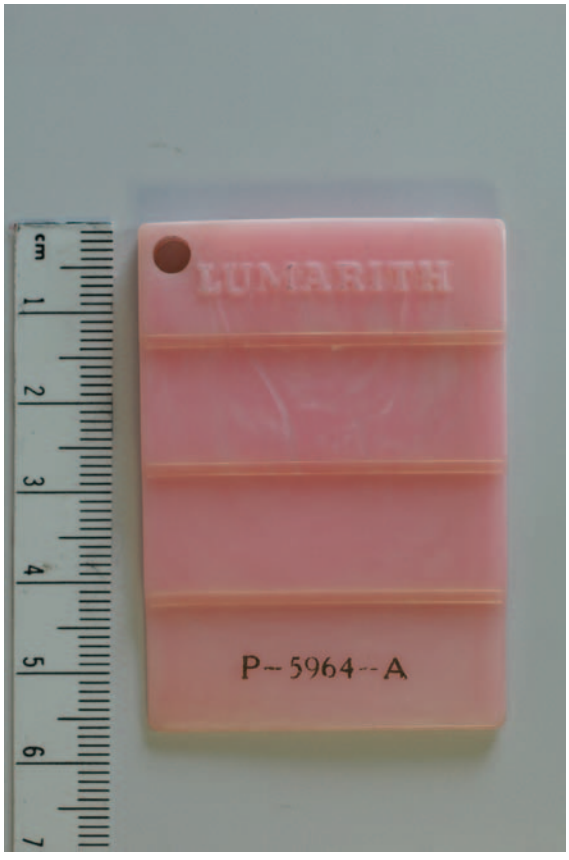

Figure 2 *Example of a coupon (Coupon 40) in good condition.*

BACKGROUND: CELLULOSE ACETATE AND 'LUMARITH' PRODUCTS

The development of cellulose acetate grew out of a commercial need to improve upon cellulose nitrate. By 1909, the Celluloid Corporation, until then a manufacturer of CELLULOID brand cellulose nitrate products, was searching for a suitable additive to reduce the flammability of Celluloid [3]. Instead they discovered a substitute in the form of cellulose acetate. Almost immediately, the Celluloid Corporation began production, and in 1910 made the first serious commercial attempt to market 'non-flammable safety film' made of cellulose acetate [4]. Development of cellulose acetate as an injection-moldable plastic to create three-dimensional objects was in commercial production by 1926 under the trade name Lumarith

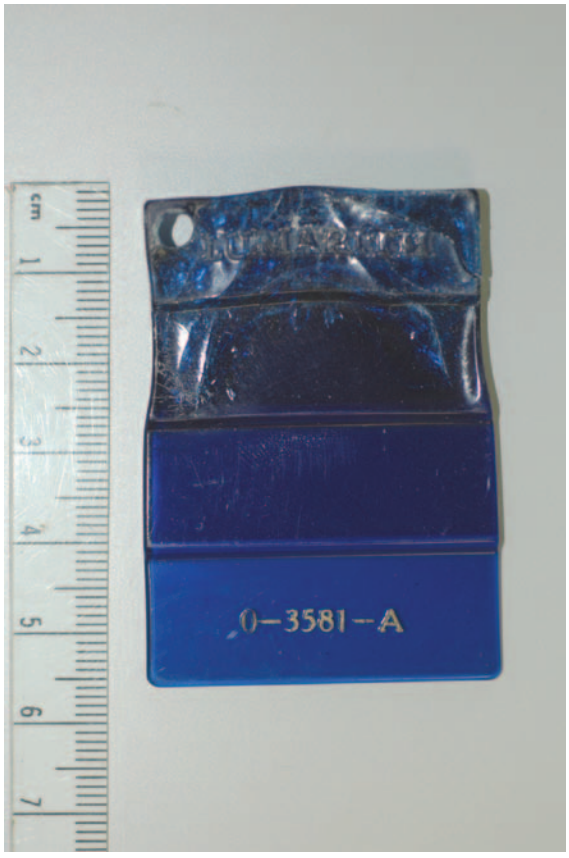

Figure 3 *Example of a coupon (Coupon 9) in an advanced stage of deterioration.*

[5]. Lumarith, described by the manufacturer as a thermoplastic colloidal or solid solution of cellulose acetate and plasticizers, with solvents, dyes and pigments [6], was produced in sheets, rods, tubes and injection-molding powders that in turn were used in the manufacture of spectacle frames, lampshades, handbags, novelties, watch crystals, radio dials, records and thousands of other everyday articles. Transparent sheets of Lumarith were used as windows for airplanes and gas masks during World War II and as non-flammable film base for motion pictures and transparencies. Transparent and colored versions quickly found popularity as toys, household implements, jewelry and spectacle frames, among many other uses.

The material came to be used in some high-temperature applications, such as lampshades, for which the flammable cellulose nitrate was an inappropriate choice. Company records suggest that specific recipes and processes were customized for individual clients in order to realize the desired mechanical properties of their finished object [5]. Recipes were modified by varying the colors, fillers, and the type and concentration of plasticizer. A stamped number at the bottom of each coupon appears to be a unique product number which imparts information about pricing, color and flow properties of the material during production. Lists of product numbers in the company records from 1936 appear to correlate each product number with a use for the plastic, such as fountain pen casings, and the name of the company for which the product was developed. Thus, it seems that the Celluloid Corporation may have developed its various Lumarith compositions on an 'as-needed' basis. Once a satisfactory product formulation was developed for one company, the specific formulation was assigned a product number that Lumarith salesmen could then market to other clients.

According to the Celluloid Corporation's company records [5], its cellulose acetate products were made from the reaction of cellulose, derived from cotton fibers, linters and/or paper, with acetic acid (ethanoic acid) or acetic anhydride (ethanoic anhydride) in the presence of sulfuric acid. The final material was a cellulose ester polymer on which hydrogen atoms of the cellulose ring were substituted with acetate groups. Unlike cellulose, cellulose acetate can be solubilized in organic solvents, and the solubility parameters depend upon the degree of acetylation. Di-acetate and tri-acetate varieties of cellulose acetate refer to the degree of acetylation of the cellulose. These two materials are very similar in terms of their mechanical properties and spectral characteristics, though they differ in their solubility in organic solvents and long-term stability.

Because cellulose acetate decomposes at temperatures lower than the softening temperature, plasticizers were added to the product in order to lower the softening temperature and improve the flow properties of the molten plastic during the injection-molding process [7]. Addition of plasticizers also modified other material properties of the final plastic, including strength, flexibility, heat distortion temperature and fire retardance [7]. Plasticizers could be incorporated into the cellulose acetate either by a solvent-casting process or by using the liquid plasticizer as a solvent, as in the case of diethyl phthalate. Plasticizers known to have been used in Lumarith include diethyl phthalate, dimethyl phthalate, triphenyl phosphate and dimethoxy ethyl phthalate [8].

In making Lumarith, the Celluloid Corporation

aimed to achieve a product that could be formed into many shapes, was durable, had minimal heat shrinkage during processing, and was clear and vibrant in color.

EXPERIMENTAL

The aim of this study was to use non-invasive and non-destructive analytical methods to identify the constituents of the Lumarith coupons, to assist in determining the factor or factors responsible for, or contributing to, the onset and progression of degradation. Exceptions to the non-invasive protocol were FTIR analysis of the liquid exuding from Coupon 9, and X-ray diffraction analysis of white crystals on the surface of one severely degraded coupon and the metal chain that linked the coupons together. All coupons were examined visually, weighed, measured and photographed at various magnifications. In addition, organic and inorganic chemical analyses were performed using a variety of complementary techniques.

Technical description and condition of the Lumarith samples

Each coupon is a solid, rectangular piece of plastic. The undegraded coupons measure approximately 3.8 × 6.3 cm. The thickness of each coupon varies from top to bottom in a series of four descending steps (Figure 2); the uppermost step of the coupon (which includes the point at which the molten plastic was injected into the mold as well as the LUMARITH logo) is *c.* 6 mm thick and each successive tier is *c.* 1.5 mm thinner than the preceding tier. The name 'LUMARITH' was embossed across the top of each coupon in raised letters during the molding process. Traces of white powder that are probably a mold-release agent remain in recessed areas along the edges of the letters (Figure 4). A unique product code (e.g., X-XXXX) is stamped onto the lower edge of each coupon. The coupons are strung together using a 35 cm metal chain through a hole at the upper right-hand corner of each coupon. The order of the coupons on the chain was documented by numbering them 1 through 49 (i.e. Coupon 4 was located between Coupons 3 and 5) to track trends in the onset, as well as the spread, of degradation.

Initial visual examination revealed that 18 of the 49 coupons in the sample kit showed some signs of degradation; three of these were severely degraded. The three most degraded samples exhibited severe cracking, distortion and shrinkage. In each of the most degraded coupons, the damage was most severe at the top of the coupon, whereas the bottom of the coupon appeared undegraded. The cracking included long open cracks that emanate from the injection point at the top of the coupon and radiate down and outward. A network of finer, crizzled cracks also was visible throughout the degraded sections. White crystalline efflorescence was visible on the surface of degrading areas (Figure 5).

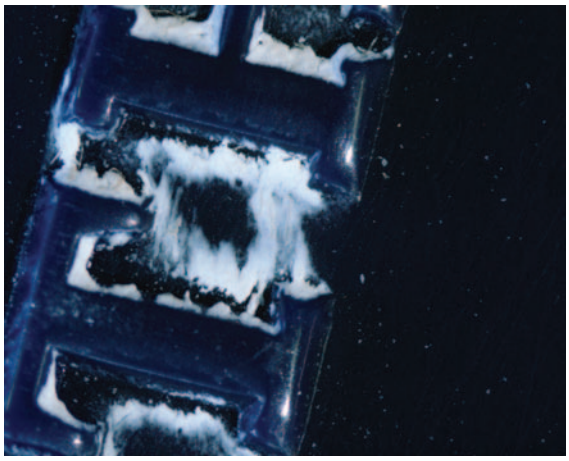

Figure 4 *White residue found in and around the logo at the top, most likely the remains of residue from a mold-releasing agent, commonly used during injection or compression molding of plastic (see Figure 15b).*

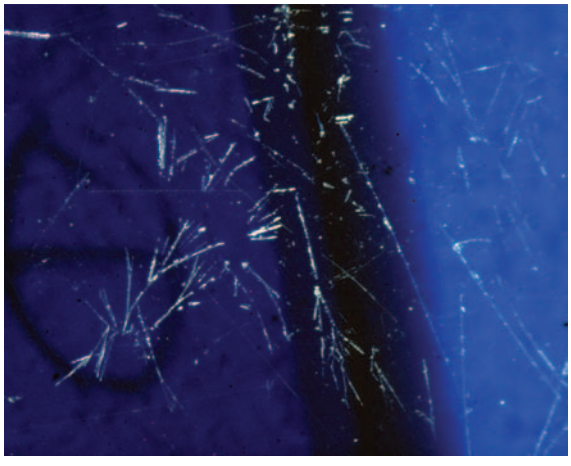

Figure 5 *Detail of Coupon 9. Triphenyl phosphate (one of three plasticizers identified in the 'Lumarith' coupons) has leached out of the cellulose acetate and redeposited as feather-like crystals on the surface of coupon (image width: 0.25 cm).*

Figure 6 *Green corrosion covers the surface of the metal ball (0.2 cm in diameter) from the nickel-plated metal chain. White flakes found in the corroded surface were identified as triphenyl phosphate by FT-Raman and XRD analysis.*

A thin film of liquid was observed on the surface of Coupon 9 (Figure 3). Some degradation was also noted on the coupons adjacent to the three that were degraded most. A brown stain that permeated the plastic near the chain hole on Coupon 1 (Figure 1) appeared to be caused by interaction with the metal of the chain.

The metal chain exhibited green-blue corrosion (Figure 6) that is concentrated on the metal at the points where the chain was in contact with the three degraded coupons and has transferred to the surface of the holes of all 49 coupons. The condition of each coupon is described in Table 1.

Fourier transform Raman spectroscopy (FT-Raman)

Components of the plastic were analyzed by FT-Raman spectroscopy using a Thermo Electron NXR FT-Raman module attached to a Thermo/Nicolet 6700 FTIR spectrometer. The Raman module incorporates a continuous wave $NdYVO_4$ excitation laser that emits at 1064 nm. The instrument employs two detectors: an electronically cooled InGaAs detector and a more sensitive germanium detector cooled with liquid nitrogen. Two beam splitters are available – an extended KBr beam splitter, and a more sensitive CaF_2 beam splitter.

Coupons were analyzed directly without sampling. Each was subjected to 256 or 512 scans. The power density of the excitation laser and the gain were adjusted for each coupon to maximize signal and minimize the potential for damage to the sample.

Fourier transform infrared spectroscopy (FTIR)

A Thermo/Nicolet 6700 FTIR spectrometer was used to identify liquid on degraded Coupon 9; white crystalline efflorescence from the Lumarith coupons; and a white deposit, suspected to be a mold-release agent, on the Lumarith company logo on one coupon. A Thermo/Nicolet Smart Golden Gate diamond attenuated total reflectance (ATR) accessory and a Centaurus FTIR microscope with diamond anvil cell were used for these analyses.

X-ray fluorescence spectrometry (XRF)

The elemental composition of the Lumarith coupons was measured using an ElvaX energy-dispersive X-ray fluorescence (XRF) spectrometer. The instrument consists of an X-ray generator (i.e. the tube), an X-ray detector, and a multi-channel analyzer (MCA). The detector is a solid state Si-pin-diode with a resolution of about 165 eV at 5.9 keV (at 1000 counts per second) with an active area of 6 mm^2. The tungsten anode X-ray tube is air-cooled and has a 140 μm beryllium end-window.

Two measurements were made for each sample. For the first analysis, samples were analyzed for 200 s (live time) at a voltage of 45 kV and current of 20 μA using an aluminum-nickel filter. These settings optimized the identification of the following elements: As, Ba, Br, Co, Cd, Cr, Cu, Mn, Fe, Nb, Pb, Rb, Se, Sr and Zn. For the second analysis, samples were analyzed for 200 s (live time) at a voltage of 10 kV and current of 30 μA using an aluminum filter. These settings facilitated the identification of low-Z elements, including Ca, Cl, K, P, S and Ti.

Scanning electron microscopy with energy dispersive spectroscopy (SEM-EDX)

Several coupons were examined and elemental maps were generated using a Hitachi S-3700N scanning electronic microscope (SEM) with a Bruker-AXS XFlash energy-dispersive spectrometer (EDX). Analyses were performed at low vacuum (100–270 Pa), with an accelerating voltage of 10 or 15 kV. The coupons were introduced into the sample chamber in their entirety with no alteration.

Table 1 *Description of 'Lumarith' coupons and elements identified by XRF analyses*

Coupon no.	Product no. (imprinted on coupon)	Color and transparency	Condition	Weight (g)	Elements detected by XRF	Condition ranking*
1	P-5965-A	pale blue/green, opaque	brown stain near hole, white silica near logo	8.87	Ca, Ti, Cu, Fe, Pb	D
2	O-2881-B	deep blue, transparent	abrasion, white silica near logo	8.63	Ca, Fe, Cu, Pb	ND
3	O-5801-A	deep blue, opaque	white bloom on back, white silica near logo	8.65	Si, Ca, Ti, Mn, Fe, Zn, Pb, Rb, Sr, Zn, Nb	ND
4	O-387	dark blue, transparent	white silica near logo, trace of brown deposits	9.11	Si, S, Ca, Fe, Cu, Pb	ND
5	O-5958-A	dark dull blue, opaque	white silica near logo, abrasion	8.91	Si, Ca, Ti, Fe, Cu, Co, Pb	ND
6	O-4005-A	ocean blue, opaque	white silica near logo, mark	8.86	P, Ca, Ti, Fe, Co, Zn, Pb	D
7	O-5724-A	medium blue, transparent	white silica near logo, abrasion, dull	8.66	Ca, Fe, Cu, Pb	ND
8	O-5743-A	dark blue, opaque	excess silica near logo, dull, abrasion	9.00	S, Ca, Ti, Fe, Cu, Zn, Pb	D
9	O-3581-A	dark blue, transparent	weeping, cracking, shrinkage	6.68	P, Ca, Fe, Cu, Pb, Br	SD (Figure 4)
10	O-5723-A	orange, transparent	excess green corrosion near chain hole	8.76	Ca, Ti, Fe, Cu, Pb	D
11	O-4621-A	light orange, transparent	white silica near logo	8.57	Ca, Fe, Cu, Pb	ND
12	O-5837-A	light yellow, transparent	visible green corrosion near chain hole	8.51	Ca, Fe, Cu, Pb	ND
13	O-2901-A	orange-yellow, translucent	visible green corrosion near chain hole	8.85	P, Ca, Ti, Fe, Cu, Pb	D
14	O-2253-A	light orange, transparent	severe cracking, severe shrinkage	5.86	P, Ca, Fe, Cu, Zn, Pb	SD
15	O-5799-A	amber, transparent	severe green corrosion near chain hole, cracking	8.93	Ca, Fe, Cu, Pb	D
16	O-5678-A	light orange, transparent	minor green corrosion near chain hole	8.79	Ca, Fe, Cu, Pb	ND
17	MO-5829-A	glitter-flecked cherry red, transparent	no noticeable degradation, fluorescence (UV)	8.96	Ca, Fe, Cu	ND
18	P-5848-A	sky blue with white marble swirl, opaque	no noticeable degradation	8.82	P, Ca, Ti, Fe, Cu, Pb	ND
19	M-5629-A	light brown with lighter brown swirls, opaque	white silica near logo, scratch marks	8.55	Ca, Ti, Cr, Mn, Fe, Cu, Pb, Sr	ND
20	M-4903-A	dark brown with light brown swirls, opaque	white silica near logo	9.11	S, Ca, Ti, Cr, Fe, Cu, As, Pb	ND
21	M-4863-A	dark red-brown with swirls, opaque	white silica near logo	8.76	S, Ca, Cr, Fe, Se, Cd	ND
22	M-4003-A	brown with lighter brown swirls, opaque	white silica near logo	8.94	Ca, Ti, Cr, Fe, Cu, Pb, Se, Cd	ND
23	O-4515-A	bright orange, transparent	no noticeable degradation	8.99	Ca, Fe, Cu, Pb	ND
24	O-2250-A	pale yellow-green, very transparent	no noticeable degradation	8.54	Ca, Ba, Fe, Cu, Pb, Sr	ND
25	O-5683-A	bright yellow-orange, very transparent	bloom, abrasion	8.99	Ca, Fe, Cu, Pb	D
26	O-4485-A	yellow-orange, transparent	severe cracking, severe shrinkage	6.03	P, Ca, Fe, Cu, Pb	SD
27	O-3717-A	yellow-orange, transparent	discoloration top left, cracking on back top	8.76	Ca, Fe, Cu, Pb	D
28	O-5820-A	plum, opaque	white silica near logo	9.24	Ca, Ti, Fe, Co, Cu, Zn, Se, Cd	ND
29	P-5847-A	pale pink with white marble swirls, opaque	noticeable stress marks radiate from top to second tier of the coupon	8.76	P, Ca, Ti, Fe, Pb, Se	D
30	PO-4002-A	metallic brown, opaque	noticeable stress marks and uneven stains	9.07	Ca, Fe, Cu, Zn	D
31	PO-5759-A	dark brown-purple, opaque	white silica near logo	8.98	Ca, Ti, Fe, Cu, Zn	ND
32	M-5721-A	purple with white marble effect, opaque	no noticeable degradation	8.72	Ca, Ti, Mn, Fe, Co, Cu, Zn, Pb	ND
33	MO-652	brown with yellow-brown swirls, opaque	cloudy	9.21	Ca, Ti, Fe, Cu, Pb	ND

Table 1 *(Continued)*

Coupon no.	Product no. (imprinted on coupon)	Color and transparency	Condition	Weight (g)	Elements detected by XRF	Condition ranking*
34	M-3984-F	deep red with lighter red swirls, opaque	excess white silica near logo	8.93	Ca,Cr, Fe, Cu, Se	ND
35	M-4634-C	bright green with white swirls, opaque	no noticeable degradation	8.51	P, Ca, Ti, Fe, Cu, Pb	D
36	O-5716-A	salmon, transparent	noticeable darkening near chain hole	8.71	Ca, Fe, Cu, Pb	ND
37	P-5845-A	teal with white marble effect, opaque	no noticeable degradation	8.72	P, Ca, Cr, Fe, Cu, Pb	D
38	M-5134-A	light sky blue with marble effect, opaque	dull darkening	8.54	P, Ca, Ti, Fe. Cu, Zn, Pb	D
39	O-5771-A	dull blue-gray, opaque	no noticeable degradation	9.00	S, Ca, Ba, Mn, Fe, Cu, Pb, Sr, Nb, Sn	ND
40	P-5964-A	pink with white swirl, opaque	no noticeable degradation	8.60	Ca, Ti, Fe, Cu, Pb	ND (Figure 3)
41	PO-5856-A	grey-green, opaque	no noticeable degradation	8.67	Ca, Cr, Fe, Cu, Ga, Pb	ND
42	O-5872	dark salmon, opaque	no noticeable degradation	9.25	Ca, Ti, Cr, Fe, Cu, Ga, Pb	ND
43	O-5815-A	hunter green, opaque	noticeable white silica near chain hole	8.68	Ca, Ti, Cr, Fe, Cu, Pb	ND
44	P-5101-A	purple and green with white swirl, opaque	no noticeable degradation	8.85	P, Ca, Ti, Fe, Cu, Pb	D
45	M-5781-A	off-white with green swirl, opaque	no noticeable degradation	8.67	Ca, Ti, Fe, Cu, Pb	ND
46	O-5810-A	dark burgundy, opaque	no noticeable degradation	8.62	S, Ca, Cr, Fe, Cu, Ga, Pb	ND
47	PO-5948-A	metallic brown, opaque	dull	9.52	P, Fe, Cu, Zn	D
48	M-5803-A	pale yellow-green, opaque	dull	8.74	Ca, Ti, Fe, Cu, Pb	ND
49	P-5849-A	mustard, opaque	no noticeable degradation	8.82	Ti, Fe, Cu, Zn, Pb	ND

Notes: Green corrosion was observed in the chain hole located on the top right corner of all 49 coupons. It resulted from close contact with the corroded nickel-plated chain. Deterioration signs appear both on the front and back of the coupons.
Metal chain: copper-zinc alloy plated with nickel, confirmed by XRF. Green corrosion deposits cover the surface of the metal beads that are in close contact with the coupons (Figure 7). The most corroded metal beads are near Coupons 9, 14, and 26. Metal beads not in direct contact with the coupons have no visible corrosion. White flakes found in association with the green corrosion were identified as TPP by FT-Raman and XRD analysis.
**SD: severe degradation, D: degradation, ND: no degradation.*

X-ray diffraction spectrometry (XRD)

Samples of white crystals on the surface of one coupon and the metal chain were submitted for analysis by XRD. The instrument used was a Rigaku D/Max Rapid Micro X-ray diffractometer with a copper X-ray source and a 0.3 mm collimator, operated at 50 kV and 40 μA for 15 minutes for maximum peak intensity. The radiation parameter is copper Kα, goniometer ki: fixed at 45°, and goniometer speed of 1°/s.

RESULTS

Weight

The average weight of the 49 coupons was 8.66 g with a standard deviation of 0.68 g. Figure 7 shows that the weights were consistent for all coupons except the three most degraded, the weight of each being 25–35% less than the average. The weight of each of these three degraded coupons diverges from the mean by more than three standard deviations (Table 1).

FT-Raman spectroscopy

Fourteen coupons, including the three most degraded, were analyzed by FT-Raman spectroscopy. The Raman spectra of the coupons match well with a prepared sample of cellulose acetate plasticized with diethyl phthalate (Figure 8). The spectra of five coupons also indicate the presence of TPP. The three degraded coupons number among these, and the concentration of TPP in these coupons is significantly greater than that found in the other two (Coupons 18 and 37), which contain very low concentrations of TPP and are not visibly degraded.

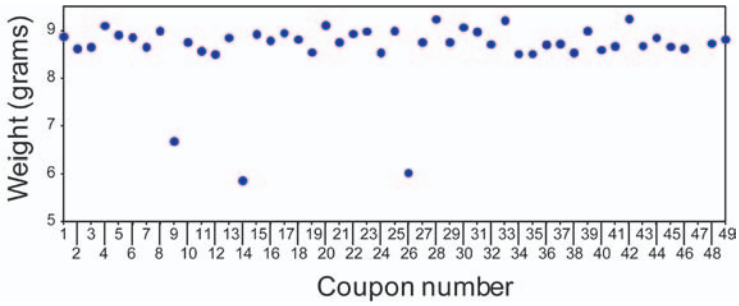

Figure 7 *Comparison of coupon number versus weight. The weight of the three most degraded coupons is nearly 30% lower than that of the undegraded coupons.*

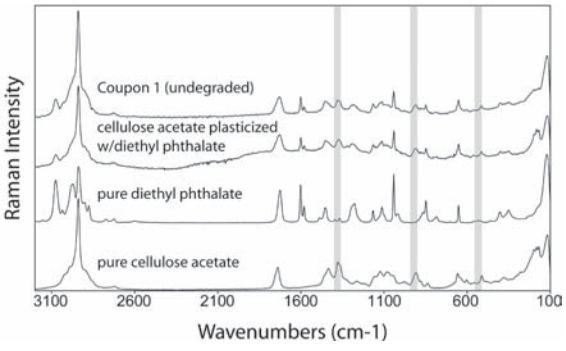

Figure 8 *(From top to bottom) FT-Raman spectra of an undegraded coupon (Coupon 1); a prepared reference of cellulose acetate plasticized with diethyl phthalate; a sample of pure diethyl phthalate; and a sample of pure cellulose acetate flake. Medium-strong peaks at 1377, 906 and 513, and a group of peaks at 200–170 cm^{-1} are unique to cellulose acetate. (Prepared reference of cellulose acetate plasticized with diethyl phthalate and the cellulose acetate reference courtesy of Dr Ray Robertson, Celanese Corporation.)*

Table 2 *FT-Raman peak table for undegraded and degraded Lumarith coupons, pure cellulose acetate, diethyl phthalate and triphenyl phosphate (Raman shift, cm^{-1})*

Undegraded coupons	Degraded coupons	Cellulose acetate	Diethyl phthalate	Triphenyl phosphate
3076	3070	2939	3075	3176
2939	2939	1739	3034	3066
1728	2895	1435	2970	3020
1601	1724	1377	2938	1593
1581	1599	1155	2900	1294
1454	1465	1122	2875	1232
1379	1377	1082	2787	1194
1300	1288	1049	2725	1174
1165	1234	987	1724	1156
1112	1165	906	1601	1076
1041	1115	837	1580	1030
910	1090	658	1489	1007
848	1041	604	1454	933
848	1028	513	1413	791
652	1007	376	1394	771
513	931	199	1367	726
	902	181	1279	616
	727	170	1165	385
	650		1113	234
	617		1041	213
	424		1018	184
	361		866	
			848	
			785	
			652	
			403	
			350	

The peak values for cellulose acetate, diethyl phthalate and TPP are presented in Table 2, along with peak values for a degraded and an undegraded Lumarith coupon. Cellulose acetate and the two plasticizers share many overlapping peaks. Peaks unique to cellulose acetate include medium-strong signals at 1377, 906 and 513 cm^{-1}. Peaks unique to diethyl phthalate include 1041, 1601 and 3075 cm^{-1}. TPP is identifiable from its strong signal at 1007 cm^{-1}, a benzene ring vibration, as well as the strong peak at 3066 cm^{-1} that overlaps with diethyl phthalate, and weaker peaks at 1232, 726–719, and 616 cm^{-1} (Figure 9).

The FT-Raman spectra compared in Figure 9 demonstrate that Lumarith plasticized with both diethyl phthalate and TPP, in this example Coupon 14, undergoes molecular changes upon degradation rather than simple leaching of plasticizer. Most noticeably, the magnitude of the strong peak at 2939 cm^{-1} decreases, broadens and shifts to lower wavenumbers. The 2939

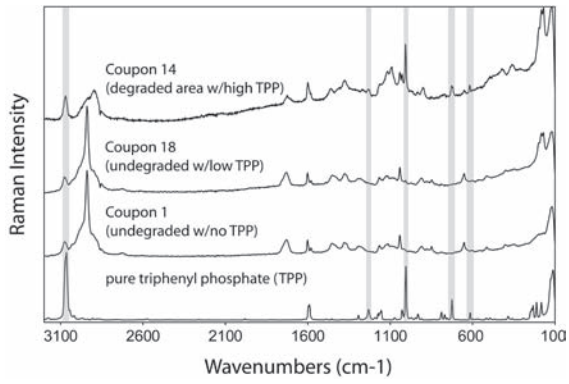

Figure 9 *(From top to bottom) FT-Raman spectra of a degraded area of Coupon 14, which contains a significant concentration of TPP; Coupon 18, which contains a very small concentration of TPP and is not degraded; Coupon 1, in which TPP was not detected and which is undegraded; and a pure sample of TPP. Peaks that are diagnostic for TPP in the coupons are shaded in gray.*

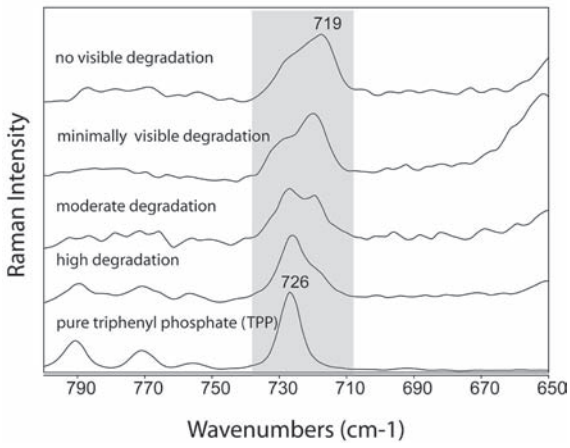

Figure 10 *FT-Raman spectra taken of four areas of Coupon 14. The uppermost was taken of an intact area of the coupon with no visible sign of degradation. The next three spectra were taken of areas in which degradation is visible: slightly degraded in the second from the top and more so in the two below. The lowest spectrum is a pure sample of TPP.*

cm^{-1} peak is associated with both cellulose acetate and diethyl phthalate.

For the most part, each coupon spectrum resembles the sum of the spectra of the components. However, some peak shift is evident in spectra of the coupons that contain TPP. Pure TPP has a peak at 726 cm^{-1}. Lumarith coupons that contain high concentrations of TPP do show a Raman peak in the general region of 726 cm^{-1}, but the exact position of this peak may vary over the range of 719–726 cm^{-1}. Furthermore, there appears to be a correlation between the shape and position of this peak and the degree of degradation visible in any one coupon. In areas without visible degradation, the main peak is centered at 719 cm^{-1} with a shoulder toward the higher wavenumber. In areas that exhibit low to moderate degradation, the main peak shifts to higher wavenumber, such that there appears a doublet at 719 and 726 cm^{-1} with varying ratio of peak areas. In the most severely degraded areas, there is a peak diminution of the lower wavenumber component to a faint shoulder and formation a distinct strong peak at 726 cm^{-1}, which is similar to the pure Raman spectrum of TPP (Figure 10). Whether the effect observed here is due to a gradual x-shift of the peak or to overlapping of two distinct peaks has not been determined. The causes of this phenomenon have been investigated and will be the subject of a separate upcoming publication.

FTIR

Analysis of a liquid on the surface of the degraded Coupon 9 resulted in spectra that are consistent with a mixture of TPP and dimethyl or diethyl phthalate (Figure 11).

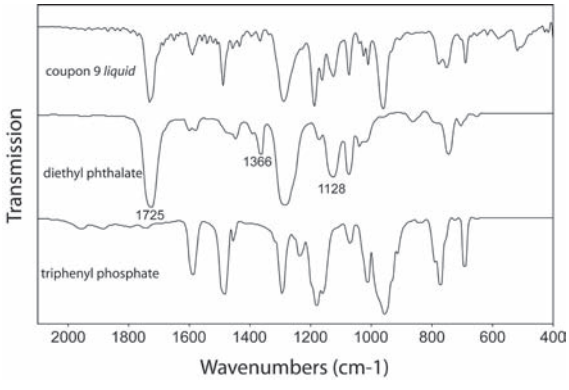

Figure 11 *(From top to bottom) FTIR spectra of liquid exuded from Coupon 9 and reference spectra of diethyl phthalate and triphenyl phosphate. The liquid and triphenyl phosphate have about ten peaks in common. Peaks at 1725, 1366 and 1128 cm^{-1} are consistent with diethyl phthalate.*

Two white residues were identified. The spectrum of the white efflorescence from a degraded surface is consistent with TPP. The FTIR spectrum of the white powder thought to be a release agent present in some recessed areas near the company logo was consistent with silica.

XRF

A list of elements identified in each coupon by XRF is provided in Table 1. With the exception of phosphorus, no correlation was observed between any element identified by XRF and degradation.

Copper, zinc and nickel were detected in the metal chain. It is likely that the white metal surface of the chain is nickel plating that covers a brass core.

SEM-EDX

SEM-EDX analysis of 13 coupons confirmed the XRF results, but with the advantage of elemental mapping, a process in which an image of the sample is overlaid with colored pixels that represent different elements relative to their location on the sample. In intact areas, phosphorus is evenly distributed in the coupon, but as degradation develops and advances, the formation of phosphorus-rich crystals is clearly visible.

The elemental maps were used to observe the different stages of degradation in Coupon 9. Figure 12a is a SEM-EDX image of the unaffected area – notably no cracks or crystals are visible near the bottom (thinnest section) of Coupon 9. Figure 12b isolates the element map for phosphorus, clearly showing that it is not migrating and is evenly distributed across this area.

Figures 13a and 13b were obtained from an area near the middle of the Coupon 9 in the second thickest tier. The degradation has begun to spread into this area. The SEM-EDX image (Figure 13a) shows a fairly smooth surface with some white areas along the left side of the image and a white scratch running vertically near the center. Also visible are some acicular/dendritic crystals in the top right and along the right side of the image. These crystals are rich in phosphorus (Figure 13b). Figures 14a and 14b also were obtained from Coupon 9, but in a thicker region closer to the top of the sample, where the degradation is more advanced. Phosphorus-rich crystals and a crack are visible in the SEM image of this area.

Figures 15a and 15b are from Coupon 26, a yellow-orange coupon that is among the most degraded of the samples. The images depict the area surrounding the 'U' in 'LUMARITH' along the top of the coupon. A fine powder is visible along the edges of the 'U', and several possible crystalline lumps are present (Figure 15a). The elemental map (Figure 15b) shows that the powder is higher in silicon and that the crystals are higher in phosphorus.

XRD

XRD analysis of the white flakes from the metal chain identified peaks consistent with TPP and paraffin wax (Figure 16) [9]. Although it is conceivable that TPP

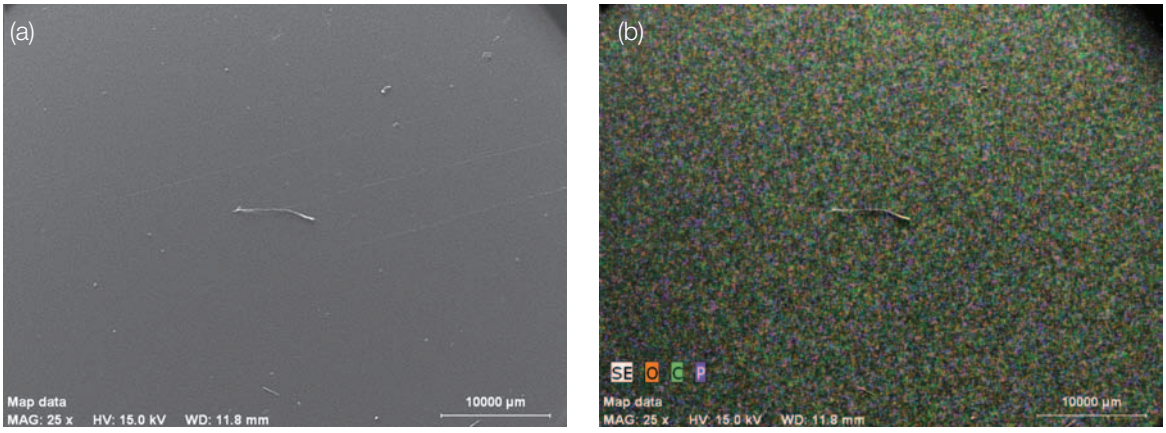

Figure 12 *Non-degraded area of Coupon 9: (a) scanning electron micrograph; and (b) elemental map of the same area, showing oxygen (orange), carbon (green), and phosphorus (purple).*

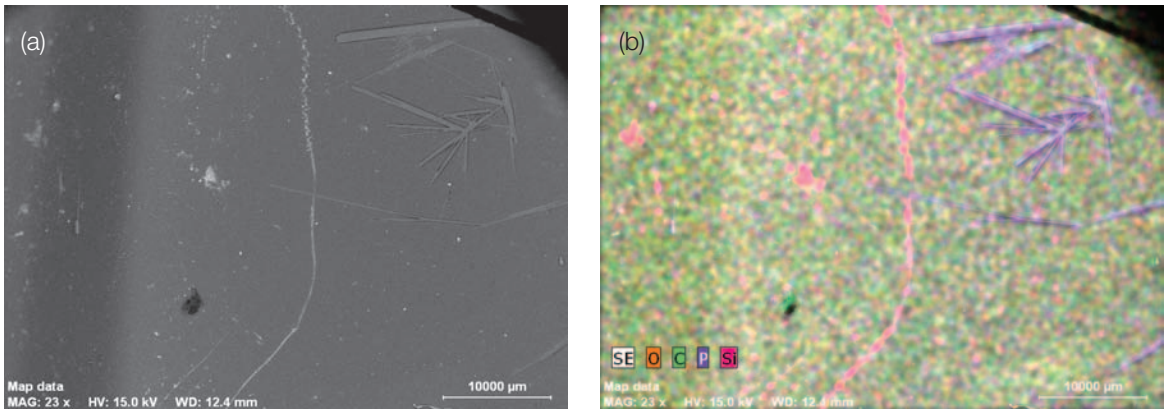

Figure 13 *An area in the upper-middle section of Coupon 9 where early signs of deterioration were detected: (a) scanning electron micrograph, showing formation of acicular crystals in the upper right area of the image; and (b) elemental map of the same area, showing the distribution of oxygen (orange), carbon (green), phosphorus (purple) and silicon (pink). Note that the crystals in the upper right area of the image have noticeable concentrations of phosphorus.*

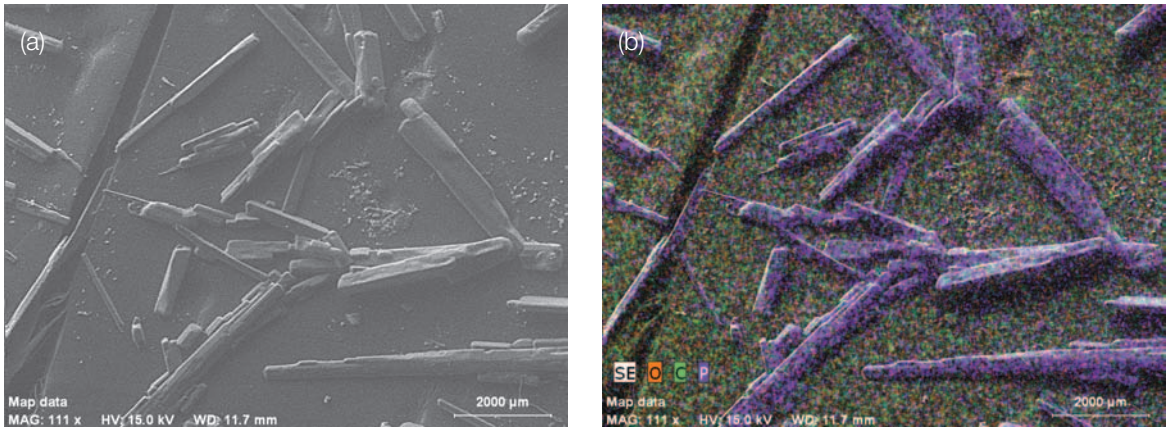

Figure 14 *The top (most degraded) section of Coupon 9: (a) scanning electron micrograph, showing well-developed, phosphorus-rich crystals and a crack; and (b) elemental map of the same area, showing oxygen (orange), carbon (green) and phosphorus (purple). The crystals are enriched in phosphorus in comparison to the surrounding area.*

could hydrolyze to diphenyl phosphate (DPP), this is not the case given that DPP was not present in the XRD pattern. Several minor phases were tentatively identified in the sample; these include copper acetate tetrahydropyrimidinone, zinc aluminum formate hydrate and/or silicon dioxide. Although copper acetate tetrahydropyrimidinone is an excellent match with the XRD reference pattern, it is not possible to account for the presence of tetrahydropyrimidinone. However, given the nature of the chain (a highly corroded nickel-plated copper chain) and the fact that it was in contact and interacting with an actively degrading cellulose acetate object, it is reasonable to assume that the identification of copper acetate is accurate. Because zinc aluminum formate hydrate and silicon dioxide share a similar crystalline structure (primarily with their major peak), it was not possible to determine which of these phases were present in the sample. Zinc aluminum formate

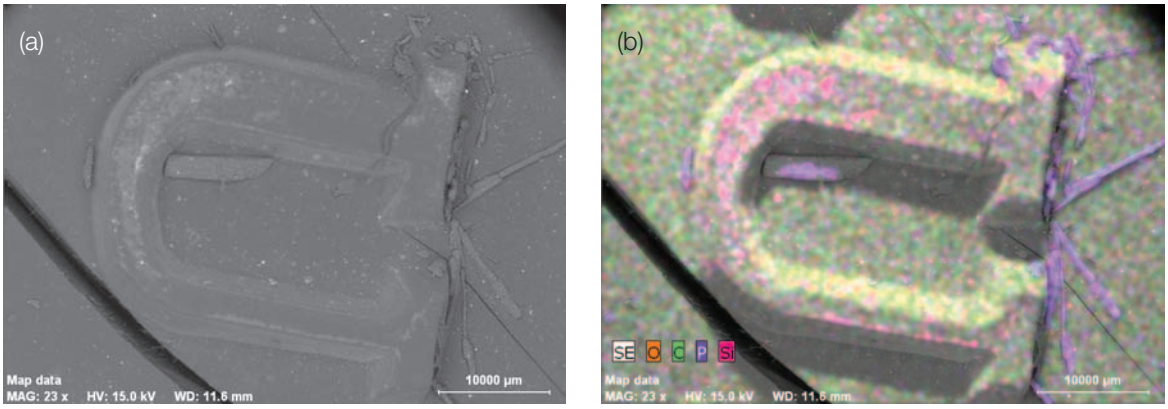

Figure 15 *The 'U' in the Lumarith logo at the top of the Coupon 26: (a) scanning electron micrograph, showing white dust in various places on the 'U', especially near the bottom and upper left corner; several cracks and crystals are also visible; and (b) elemental map of the same area, showing oxygen (orange), carbon (green), phosphorus (purple) and silicon (pink). The white dust on the surface of the coupons is silica, probably the release agent used in the molding process (see Figure 4). The presence of these phosphorus-rich crystals supports the hypothesis that plasticizer loss is occurring in the degrading coupons.*

hydrate and silicon dioxide could result from (1) the presence of zinc on the chain; (2) the possibility of dirt, dust and grime on the chain (e.g. Si, Al, O, Fe); or (3) the fact that silicon was used as a release agent during manufacture of the coupons. Inconclusive identifications are denoted in Figure 16 by a '?'.

DISCUSSION AND CONCLUSIONS

Of the 49 Lumarith color samples, three are severely degraded and 15 others exhibit slight signs of degradation. The most degraded coupons exhibit shrinkage, cracking, efflorescence of white crystals of triphenyl phosphate and, in the case of Coupon 9, the appearance of a thin film of diethyl phthalate plasticizer on the plastic surface. The 15 coupons that exhibit degradation to a lesser degree show some localized fine cracks, areas of discoloration, and/or subtle changes in surface gloss; however, these coupons are intact and of similar weight to those coupons for which no degradation was noted.

All 49 coupons share a similar composition of a cellulose acetate polymer and diethyl phthalate plasticizer. Although the coupons contain a variety of colorants, opacifiers and, in one coupon, pieces of glitter, there does not seem to be any correlation between these components and observed degradation. The one apparent feature that the three severely degraded coupons share is the presence of triphenyl phosphate – a plasticizer that is known to have been used in cellulose acetate to impart fire retardancy, moisture resistance and other qualities.

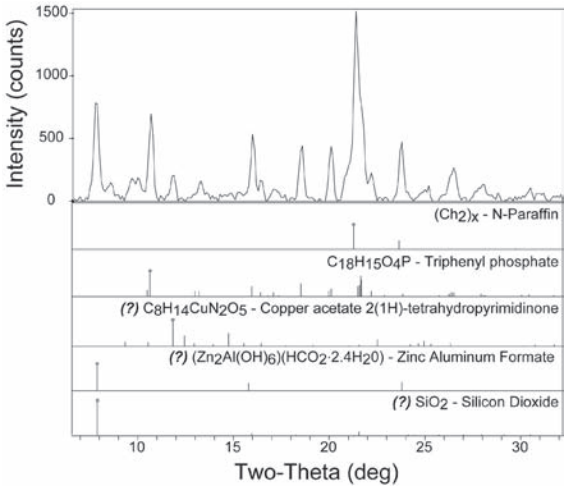

Figure 16 *XRD results from the analysis of the white crystal removed from the corroded chain. The white crystal was identified as triphenyl phosphate using FT-Raman, and as phosphorus-containing by low vacuum SEM. Triphenyl phosphate has leached from the degraded Lumarith coupons, migrated to the metal chains and possibly corroded the metal balls that chained the Lumarith coupons together.*

Triphenyl phosphate was identified definitively by FT-Raman spectroscopy, both in the degraded plastic coupons and as white crystals on the surface. TPP was also detected in a few coupons that exhibited no sign of degradation. However, the concentration is much less

than in the degraded examples, and the strongest peak for TPP at 1007 cm^{-1} is barely visible in the spectrum. The inorganic elemental composition of each coupon was identified by XRF, and the distribution of phosphorus among the coupons agrees with the FT-Raman data. TPP was also identified by XRD on the metal chain that bound the coupons together.

Of the samples that show some sign of degradation but do not contain TPP, six out of seven are adjacent to a degrading coupon that contains TPP. Coupon 18 is the single TPP-containing coupon that has not yet begun to exhibit signs of degradation. These facts strongly suggest that TPP plays a role in the degradation observed in these objects and that the degree of degradation is correlated with TPP concentration.

Other researchers have studied the effects of TPP on cellulose acetate [10–12], mainly focusing on cellulose triacetate films (both for photography and paper lamination), rather than three-dimensional injection-molded forms.

Wilson and Forshee identified the benefits of TPP in paper lamination as 'increasing the hardness and durability of the film', even at a suggested concentration of 5% by weight [10]. Allen et al. stated that '(p)lasticizer is incorporated in cellulose triacetate photographic film in order to render the base flexible' and suggested that '(b)oth the plasticizer and the emulsion layer impart some stability to the film substrate, probably associated with their ability to neutralize and scavenge the acid' [11]; a concentration of 20% TPP is indicated. Some further effects of TPP are noted by Allen et al.: 'It is seen that moisture regain is markedly inhibited by the plasticizer and this is consistent with a better retention of viscosity. The TPP is therefore imparting some protection to the polymer film probably by undergoing hydrolysis'; and 'The presence of acetic acid … is also seen to markedly accelerate the loss of the plasticizer… These results are interesting since they relate closely to what is observed in real archival condition where the process of acetic acid release is the precursor to plasticizer loss' [11]. Wilson and Forshee make clear that for the use of cellulose acetate in lamination, inclusion of an antioxidant and an acid acceptor is necessary for stability, state that unplasticized cellulose acetate is more stable than plasticized, and suggest that TPP can be left out of the plastic film if desired (and when included, recommend it only at 5%) [10]. Allen et al. also say 'it appears that diffusion or migration of the plasticizer is more associated with hydrolysis and deacetylation of the cellulose triacetate film. Under these conditions the plasticizer would be incompatible with the substrate and therefore migrate to the film surface and crystallize' [11]. Shinagawa and colleagues conducted accelerated aging tests on cellulose triacetate film and investigated the effects of TPP on its deterioration [12]. According to their study, cellulose triacetate is fairly stable, even at elevated humidity and temperature, but it is very vulnerable to attack by acids. They assert that TPP, incorporated into cellulose acetate film, readily hydrolyzes in wet conditions to form a more acidic diphenyl phosphate and phenol. When present in sufficient concentration, the diphenyl phosphate increases the acidity of the plastic and catalyzes rapid degradation of cellulose acetate. In the current study of Lumarith, triphenyl phosphate was identified on the metal chain that bound the coupons, using XRD. It is also suspected that a growth in a sharp peak in the 1025–1028 cm^{-1} region of the FT-Raman spectra of the coupons that contain a relatively high concentration of TPP is associated with increased phenol concentration in degrading Lumarith coupons.

Given the above descriptions of cellulose acetate degradation and interaction with TPP, a possible progression of the degradation of the Lumarith coupons might begin with the catalyzation of cellulose acetate by some undetermined factor, such as elevated heat, humidity, ultraviolet light, and/or repeated cycling of any or all of these variables. Acetic acid is then released as a product of the degradation, and the physical structure of the coupons becomes visibly changed, with shrinkage, cracking, distortion and efflorescence all evident.

Cracking and warping of the degraded Lumarith coupons appears to result from shrinkage brought about by deacetylation, leading to acetic acid loss and plasticizer loss, and scission of the cellulose acetate polymer chain. Each of the most degraded coupons has shrunk by nearly 30% relative to the undegraded coupons. The visual appearance of the warped and cracked coupons also suggests shrinkage. The warping is primarily a narrowing of the coupon width at its center. The major cracks that run through the degraded coupons run from the injection point at the center of the top edge and radiate down and outward. They appear to run parallel to the polymer chain. Loss of acetyl side groups and plasticizer from between the polymer strands would presumably result in this kind of crack pattern. Analysis of Coupon 9 with A-D Strips indicates that acidic vapors are emanating from the coupon, and given the analyzed composition of the coupon the acid is probably acetic acid. (A-D Strips are paper test strips that can detect acid vapor and are commonly used to monitor cellulose acetate film deterioration.) Other types of cracking, particularly the smaller network of cracks that resembles

crizzling in glass, may be caused by scission of the polymer chain. The glycosidic linkages that connect the cellulose chain are broken in acidic conditions resulting in a cracked, brittle and weakened material.

The data suggest that TPP in cellulose acetate plastic is a risk factor for degradation. This study shows that cellulose acetate plastics can be surveyed non-invasively using XRF, FT-Raman and FTIR, all of which are available as portable instruments. Also, it seems that FT-Raman could be used to evaluate the degree of deterioration in at-risk cellulose acetate plastics. In FT-Raman, the increased intensity of the 726 cm^{-1} peak of TPP as cellulose acetate degradation increases may indicate a loss of compatibility between TPP and cellulose acetate which has resulted in TPP migration out of the plastic.

This preliminary investigation is the beginning of much-needed systematic study to identify properly the components of cellulose acetate plastics [13–17], to isolate and measure the markers of degradation, to study the mechanisms that trigger the deterioration, and to design the best practices for storage and exhibition.

ACKNOWLEDGEMENTS

The authors would like to acknowledge Richard Barden (NMAH) and Ann Seeger (NMAH) for their support of plastic preservation research with NMAH collections; the Celanese Corporation for providing access to some of their historic archives and, in particular, Dr Ray Robertson for sharing his knowledge of cellulose acetate processing and samples of material; Doug Nishimura and Dr James Riley at Image Permanence Institute, Rochester Institute of Technology for sharing their knowledge of cellulose acetate deterioration in film; and Robert Koestler (MCI) and Paula DePriest (MCI) for their support of modern materials research. Walter Hopwood (MCI) performed the Fourier transform infrared spectroscopy. Special thanks to the Kress Foundation for supporting Mary Coughlin's conservation fellowship in 2005–2006 on the plastic survey project at NMAH, which laid the foundation and focus for this research.

SUPPLIERS

A-D Strips: Image Permanence Institute, Rochester Institute of Technology, www.imagepermanenceinstitute.org/shtml_sub/cat_adstrips.asp (accessed 6 April 2009)

REFERENCES

1 Coughlin, M., *Preservation and Storage of Plastics*, Samuel H. Kress Fellowship Report, Preservation Services, National Museum of American History, Smithsonian Institution (2006).
2 Williams, R.S., 'Care of plastics: Malignant plastics', *WAAC Newsletter* **24**(1) January 2002, http://palimpsest.stanford.edu/waac/wn/wn24/wn24-1/wn24-102.html (accessed 6 October 2008).
3 Meikle, J., *American Plastic*, Rutgers University Press, New Brunswick (1995).
4 Anderson, E.H., and Thompson, C.W., 'Plastics – a debutante industry', *Southern Economic Journal* **17**(2) (1950) 174–186.
5 Harding, R.S., and Etu, E.S., *CELLULOID Corporation Records* (1892–1935) #9 (3 cu. ft.: 2 DB, 1 F/O), NMAH Archives Center.
6 Boehmer, G.H., *Celluloid – Grand Daddy of 'Em All*, The Celluloid Corporation, Newark, New Jersey (1935).
7 Brydson, J.A., *Plastic Materials*, 7th edn, Butterworth-Heinemann, Oxford (1999) 613–634.
8 Lumarith Archives, Celanese Corporation, Narrows, Virginia.
9 *Powder Diffraction File – Organic and Organometallic Phases Search Manual for Experimental Patterns*, Sets 1–55, International Centre for Diffraction Data, Newton Square, PA (2005).
10 Wilson, W.K., and Forshee B.W., *Preservation of Documents by Lamination*, National Bureau of Standards Monograph, Government Printing Office, Washington, DC (1959).
11 Allen, N.S., Edge, M., Appleyard, J.H., Jewitt, T.S., Horie, C.V., and Francis, D., 'Acid-catalysed degradation of historic cellulose triacetate cinematographic film: Influence of various film parameters', *European Polymer Journal* **24**(8) (1988) 707–712.
12 Shinagawa, Y., Murayama, M., and Sakaino, Y., 'Investigation of the archival stability of cellulose triacetate film: The effect of additives to CTA support', in *Polymers in Conservation,* ed. N.S. Allen, M. Edge and C.V. Horie, Royal Society of Chemistry, Cambridge (1992) 139–149.
13 Shashoua, Y.R., *Inhibiting the Deterioration of Plasticized Poly (Vinyl Chloride): A Museum Perspective*, PhD dissertation, Technical University of Denmark (2001).
14 Allen, N.S., 'Action of light on dyed and pigmented polymers', in *Polymers in Conservation*, ed. N.S. Allen, M. Edge, and C.V. Horie, Royal Society of Chemistry, Cambridge (1992) 193–213.
15 Coxon, H. C., 'Practical pitfalls in the identification of plastics', in *Saving the Twentieth Century: The Conservation of Modern Materials*, ed. D.W. Grattan, Canadian Conservation Institute, Ottawa (1993) 395–406.
16 Quye, A., and Williamson, C., *Plastics: Collecting and Conserving*, NMS Publishing Ltd., Edinburgh, (1999).
17 Reilly, J.A., 'Celluloid objects: Their chemistry and preservation', *Journal of the American Institute for Conservation*, **30**(2) (1991) 145–162.

AUTHORS

Jia-sun Tsang is a senior paintings conservator at the Smithsonian's Museum Conservation Institute, USA. She has a MS degree in art conservation from the Winterthur/University of Delaware (USA) program in art conservation and a MS degree in chemistry from Bowling Green State University, USA. Her research interests include non-destructive instrumental analysis and modern materials and varnishes. *Address: Smithsonian Museum Conservation Institute (MCI), Suitland, MD, USA. Email: tsangj@si.edu*

Odile Madden is a research scientist at the Smithsonian's Museum Conservation Institute, USA. She received a MA degree in history of art and archaeology and a diploma in conservation from New York University, USA in 2001 and is currently completing her PhD in materials science and engineering at the University of Arizona, USA. Her research interests include technical art history, characterization of polymeric materials, challenges surrounding pesticide residues on cultural materials, and Raman spectroscopy. *Address: as Tsang. Email: maddeno@si.edu*

Mary Coughlin is an objects conservator at the Smithsonian's National Museum of American History. She received a Samuel H. Kress Fellowship to survey plastic collections at NMAH after she graduated from the Winterthur/University of Delaware program in art conservation in 2005. *Address: Smithsonian National Museum of American History (NMAH), Washington, DC, USA. Email: coughlinm@si.edu*

Anthony Maiorana was an intern at the Smithsonian's Museum Conservation Institute and is currently pursuing a BS degree in chemistry at the University of Maryland at College Park, USA. His main interests are in instrumental methods of analysis. *Address: Department of Chemistry, University of Maryland, College Park, MD, USA. Email: maioranaa@si.edu*

Judy Watson is a physical scientist at the Smithsonian's Museum Conservation Institute. She received a BSc (Hons) in archaeological science from the University of Bradford, UK. Her research interests include the use of minimally destructive analytical techniques in conservation. *Address: as Tsang. Email: watsonj@si.edu*

Nicole C. Little is a physical scientist at the Smithsonian's Museum Conservation Institute. She received MA and BA degrees from the University of Missouri at Columbia, USA. Her research interests include the use of XRD and LA-ICP-MS to study cultural materials. *Address: as Tsang. Email: littlen@si.edu*

Robert J. Speakman is a physical scientist and head of technical studies at the Smithsonian's Museum Conservation Institute. His research interests include the application of ICP-MS, XRF and neutron activation analysis to the study of cultural materials. *Address: as Tsang. Email: speakmanj@si.edu*

Résumé *— Les objets manufacturés en acétate de cellulose constituent un des groupes les plus problématiques de matières plastiques de la collection du National Museum of American History (NMAH) de la Smithsonian Institution. Afin de mieux comprendre la dégradation de l'acétate de cellulose, on a étudié au Museum Conservation Institute (MCI) de la Smithsonian Institution, par des techniques les moins invasives possibles, une trousse de représentant des ventes constituée de coupons d'acétate de cellulose colorés moulés par injection de marque Lumarith fabriqués au début du XX^{e} siècle par la Celluloid Company, et faisant aujourd'hui partie de la collection du NMAH. La trousse comprend 49 coupons de plastique dont la couleur, la transparence, la composition chimique et l'état de dégradation varient. Les résultats d'analyse ont été comparés avec les documents de la Celluloid Company conservés au centre d'archives du NMAH et à ceux de Celanese Corporation à Narrows, en Virginie, afin de déterminer les causes de l'état de préservation actuel. On discute des causes possibles de la dégradation de certains coupons, et on propose des méthodes pour identifier les objets en acétate de cellulose à risque et pour détecter les premiers signes de dégradation.*

Zusammenfassung *— In den Sammlungen des National Museum of American History (NMAH) des Smithonian Instituts stellen Objekte aus Celluloseacetat die problematischste Gruppe von Kunststoffen dar. Um den Abbau des Celluloseacetats besser verstehen zu können, wurde am Museum Conservation Institute (MCI) des Smithonian Instituts die Mustersammlung für Handlungsreisende der Marke 'Lumarith', bestehend aus spritzgeformten, farbigen Celluloseacetatproben mit minimalinvasiven Mmthoden untersucht, der im frühen 20. Jahrhundert von der Celluloid Company hergestellt worden war. Der Mustersatz*

enthält 49 Plastiktafeln, die sich in Farbe, Transparenz und chemischer Zusammensetzung unterscheiden – und heute höchst unterschiedlich erhalten sind. Die Analysenergebnisse wurden mit Aufzeichnungen der Celloloid Company im NMAH Archives Center and Celanese Corporation in Narrows, Virginia verglichen, um so den Ursachen der heutigen Zustände der einzelnen Proben auf den Grund zu kommen. Die möglichen Ursachen werden diskutiert. Es werden Methoden vorstellt, Objekte aus Celluloseacetat zu identifizieren, die mit hohem Risiko behaftet sind und frühe Anzeichen von Abbaureaktionen zu entdecken.

***Resumen** — Los objetos manufacturados con acetato de celulosa constituyen uno de los grupos de plásticos más problemáticos en las colecciones de la Smithsonian Institution en el National Museum of American History (NMAH). Para comprender mejor la degradación del acetato de celulosa, un "set de muestras de vendedor" de la marca ´Lumarith´, moldeados por inyección, muestras de color de acetato de celulosa manufacturadas por la Celluloid Company a comienzos del siglo XX y actualmente en la colección del NMAH, fueron estudiadas utilizando técnicas analíticas minimamente invasivas en el Museum Conservation Institute (MCI) del Smithsonian Institution. El kit incluye 49 muestras que varían en color, transparencia, composición química y grado de degradación. El resultado de los análisis fueron comparados con los archivos de la Celluloid Company en el NMAH Center and Celanese Corporation en Narrows (Virginia), para determinar las causas del nivel de conservación o degradación. Las posibles razones de por qué algunas de las muestras se degradaron han sido sometidas a discusión, se proponen métodos para identificar los objetos de acetato de celulosa a riesgo de degradación y para detectar la degradación con anticipación.*